

Laccase-conjugated amino-functionalized nanosilica for efficient degradation of Reactive Violet 1 dye

Mayur Gahlout¹ · Darshan M. Rudakiya¹ · Shilpa Gupte² · Akshaya Gupte¹

Received: 12 October 2016 / Accepted: 4 August 2017 / Published online: 8 August 2017
© The Author(s) 2017. This article is an open access publication

Abstract Immobilization of enzyme with nanostructures enhances its ideal characteristics, which may allow the enzyme to become more stable and resistant. The present investigation deals with the formulation of laccase nanosilica conjugates to overcome the problems associated with its stability and reusability. Synthesized nanosilica and laccase nanoparticles were spherical shaped, with the mean size of 220 and 615 nm, respectively. Laccase nanoparticles had an optimum temperature of 55 °C and pH 4.0 for the oxidation of ABTS. Laccase nanoparticle retained 79% of residual activity till 20th cycle. It also

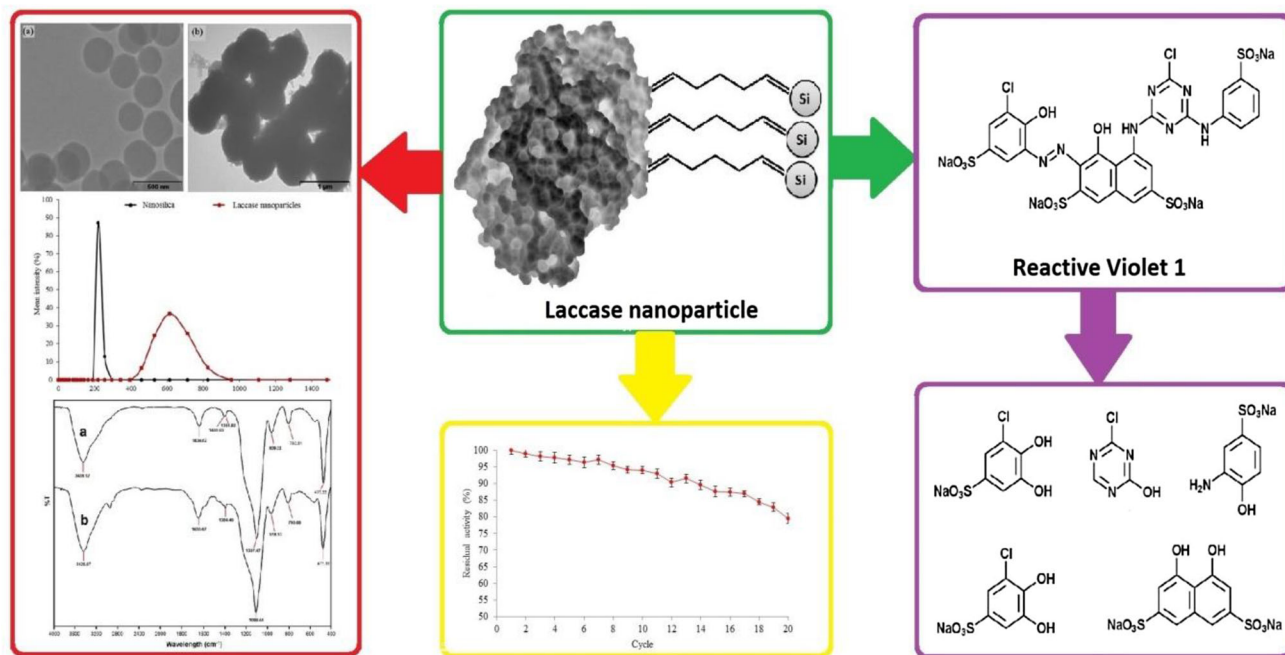
showed 91% of its initial activity at lower temperatures even after 60 days. Laccase nanoparticles were applied for Reactive Violet 1 degradation wherein 96.76% of decolourization was obtained at pH 5.0 and 30 °C within 12 h. Toxicity studies on microbes and plants suggested that the degraded metabolites were less toxic than control dye. Thus, the method applied for immobilization increased storage stability and reusability of laccase, and therefore, it can be utilized for efficient degradation of azo dyes.

✉ Akshaya Gupte
akshaya_gupte@hotmail.com

¹ Department of Microbiology, Natubhai V. Patel College of Pure and Applied Sciences, Vallabh Vidyanagar, Anand, Gujarat 388 120, India

² Ashok and Rita Patel Institute of Integrated Study and Research in Biotechnology and Allied Sciences, New Vallabh Vidyanagar, Anand, Gujarat 388 121, India

Graphical Abstract



Keywords Biocatalyst · *Ganoderma cupreum* AG-1 · Laccase nanoparticle · Nano-immobilization · Reactive Violet 1

Introduction

Enzymes catalyse more specific reactions inside living systems under mild conditions; therefore, they are efficient alternate for chemical catalysts [1]. The economy of biocatalytic process can be improved by enzyme reusability and stability by means of immobilization [2, 3]. The challenges of using immobilized enzymes are identifying new matrix materials with appropriate structural characteristics, such as morphology and surface functionality [4].

Recently, carbon nanotubes, nanosized polymer beads, and metal nanoparticles are utilized as immobilization matrices of enzymes [5]. The use of nanomaterials not only offers advantages such as large surface area, increased mechanical strength, and effective enzyme loading, but also exhibits high catalytic efficiency [6, 7]. Enzyme nano-immobilization can be performed by either physical or chemical modification. Although physical nano-immobilization leads to weaker interaction with enzymes, conformation of the enzyme is unaffected. Chemical nano-immobilization method changes the enzyme conformation, but it provides the strong covalent bond formation. 3-Aminopropyltriethoxysilane (APTES) is the aldehyde anchoring chemical, which is subsequently attached and formed covalent bond. This modification provides strong

cross-linking with protein amino surface with nanoparticles. The catalytic efficiency of an enzyme decreases due to the steric effects, limited freedom of active site, and diffusion barriers when enzyme conjugated with nanostructures [8, 9]. In addition, the binding affinity of peroxidase was decreased by immobilizing it on graphene (graphane) oxide by electrostatic interactions [8]. However, the effect of nanomaterials, substrate acted on enzyme activity, and interface nature between enzyme and nanomaterials has not been fully elucidated [10].

Laccases (E.C. 1.10.3.2) catalyse the removal of hydrogen atom from hydroxyl group of *o*- and *p*-substituted mono-phenolic and poly-phenolic substrates and from aromatic amines by one electron abstraction to form free radicals as well as capable of further reaction such as depolymerisation, re-polymerization, demethylation, or quinone formation [11, 12]. Immobilized laccase has a wide range of commercial applications such as formulation of biosensors and biofuel cells, toxic pollutant degradation, and transformation of industrially and medicinally important compounds [4, 13–15]. Laccases have been successfully immobilized with nanomaterials such as nanoparticles, nano-composite, carbon nanotubes, and nanogels [16–18].

Laccase nano-immobilization is a promising strategy for recovering laccase on amino-functionalized nanosilica. The present study is aimed to fabricate and characterize laccase-conjugated amino-functionalized nanosilica. Furthermore, prepared nano-biocatalyst was applied for the degradation of Reactive Violet 1 (RV 1) dye. Based on

several analytical procedures such as UV–visible spectrophotometry, HPTLC, and GC–MS/MS analysis, we demonstrated the produced nano-biocatalyst was efficient for decolourizing and degrading RV 1 dye. Toxicity assessment of RV 1 dye and degraded metabolites were also evaluated on microbes and on plants.

Materials and methods

Chemicals

2, 2-Azino-bis (3-ethylbenzthiozoline-6-sulphonic acid) (ABTS), tetraethyl orthosilicate (TEOS), APTES, and Sephadex G-75 were purchased from Sigma-Aldrich (St. Louis, USA). Fungal media, agar–agar, and other chemicals were purchased from Hi-media Labs. (Mumbai, India). RV 1 dye was procured from Meghmani Enterprise Pvt. Ltd. (Ahmedabad, India). All other reagents used were of analytical grade with highest purity.

Laccase production and purification

Solid-state fermentation strategy was used for laccase production using *Ganoderma cupreum* AG-1. An Erlenmeyer flask containing wheat straw (5 gm) was moistened with Asther's medium to give a final substrate to moisture ratio of 1:4 [19]. Actively grown fungal mycelia (5 agar plugs; 8 mm diameter) was inoculated on moistened wheat straw and incubated it for 16 days at 30 °C. Extrudates were extracted by squeezing fermented wheat straw using muslin cloth and centrifuged at 8000 rpm and 4 °C for 15 min. The obtained supernatant was precipitated using ammonium sulfate saturation procedure. Furthermore, precipitated protein was dialyzed overnight in Na-acetate buffer and purified using gel filtration chromatography (Sephadex G-75) at pH 5.0 (Na-acetate buffer, 50 mM).

Laccase assay

Laccase assay was performed by incubating purified laccase (100 µl) with ABTS (1 mM, 100 µl) in 800 µl of Na-acetate buffer (50 mM, pH 5.0). The rate of substrate oxidation was monitored for purified and laccase nanoparticle at 420 nm ($\epsilon = 36,000 \text{ cm}^2/\text{M}$) in a UV–visible spectrophotometer following the method described by Rudakiya and Gupte [20]. One unit of enzyme activity (U) is defined as the amount of enzyme oxidizes 1 µM of ABTS per min.

Laccase nanoparticle preparation

The nanosilica was chemically synthesized according to the method described by Stöber et al. [21]. Preparation of nanosilica was carried out by mixing TOES (4 ml) and NH_4OH (3.3 ml, 24% w/v) in ethanol (47 ml) at 20 °C for 24 h with moderate stirring. The resulting suspension was transferred to filtration assembly equipped with cellulose filtration membrane (cut off; 50 kDa) and washed thoroughly with water. With this suspension, APTES (300 µl) was added and reaction was maintained under vigorous stirring for 20 h. Prepared suspension was washed three times with Sorenson's phosphate buffer (pH 7.0) and collected in the pellet form by centrifuging it for 3 min at 10,000 rpm. After washing step, pellet of nanosilica was dried under reduced pressure and produced nanoparticles are called amino-functionalized nanosilica.

Dried amino-functionalized nanosilica (300 mg) was incubated with glutaraldehyde solution (250 µl, 50% v/v) in Sorenson's phosphate buffer (40 mM, pH 7.0) under stirring condition. Glutaraldehyde-activated nanosilica (100 mg) was washed twice with the same buffer and incubated with different concentration of purified laccase (100–800 µg) at 4 °C for 12 h. Laccase cross-linked amino-functionalized nanosilica was called as laccase nanoparticles. Immobilization yield of laccase nanoparticle for each laccase concentration was calculated by Huang et al. [22], which is defined by the following equation:

$$\text{IY \%} = \text{PB} / \text{PU} \times 100, \quad (1)$$

where IY is immobilization yield, PU is Protein used for immobilization, and PB is Protein bound to a nanoparticle; the amount of bound proteins were evaluated indirectly by measuring the quantity of protein remaining in washing solution by Lowry's method [23].

Characterization of laccase nanoparticles

Structural and functional characterization

Structural elucidation of nanosilica and laccase nanoparticles was acquired using microscopic, spectroscopic, and light scattering techniques. The size and shape of nanosilica and laccase nanoparticles were analysed using transmission electron microscopy (Tecnai 20, Philips, Holland). The interaction of laccase with amino-functionalized nanosilica was studied by Fourier Transform Infrared Spectroscopy (Spectrum GX, Perkin Elmer, USA). The average size of nanosilica and laccase nanoparticles was observed using dynamic light scattering analyzer (Zetasizer S-90, UK).

Temperature and pH optima

Temperature optimum was examined by incubating the purified laccase and laccase nanoparticles in Na-acetate buffer (50 mM, pH 5.0) at different temperatures (30–70 °C). The pH optima of purified laccase and laccase nanoparticles were determined by monitoring the oxidation of ABTS in the pH range from 2.0 to 8.0 at 30 °C. Na-acetate (50 mM, pH 3–5) and Na-phosphate (50 mM, pH 6–8) buffers were used to maintain the pH. Residual activities of purified laccase and laccase nanoparticles were measured after 1 h of incubation.

Temperature and pH stability

Thermal stability of purified laccase and laccase nanoparticles was determined at different temperatures (30–70 °C) in Na-acetate buffer (50 mM, pH 5.0) for 24 h. The pH stability was studied by incubating laccase nanoparticles and purified laccase in Na-acetate buffer at different pH values (3.0, 4.0, and 5.0) for 24 h at 30 °C. Residual activities were measured periodically at an interval of 4 h under standard assay conditions.

Storage stability and reusability

Purified laccase and laccase nanoparticles were stored at 4 and –20 °C and residual activities were measured periodically at an interval of 10 days for 60 days under standard assay conditions. Reusability of laccase nanoparticles (100 mg) was determined by incubating it with ABTS in Na-acetate buffer at 30 °C for 3 min. Operational stability were carried out for 20 cycles wherein samples were withdrawn after an interval of 3 min and absorbance was measured at 420 nm. Laccase nanoparticles were collected by centrifuging (10,000 rpm, 10 min) and washing twice with Na-acetate buffer. Subsequently, washed laccase nanoparticles were re-suspended in a fresh substrate solution and assayed subsequently.

Kinetic studies of laccase nanoparticle

The kinetic parameter of purified laccase and laccase nanoparticles was determined at 30 °C using ABTS (0.05–100 mM) in Na-acetate buffer (50 mM, pH 5.0). Kinetic parameter K_m and V_{max} were obtained using Line weaver-Burk plots. All assays were performed in triplicates.

RV 1 dye decolourization experiments

Aqueous solution of RV 1 dye (1000 mg/l) was mixed in Na-acetate buffer (50 mM, pH 5.0) to give a final

concentration of 100 ppm in experimental flask. The reaction was initiated by addition of purified laccase (2000 U) and laccase nanoparticles (2000 U), and mixture was incubated for 12 h at 30 °C. The samples were withdrawn periodically at an interval of 2 h and decolourization was analysed spectrophotometrically using UV–visible spectrophotometer. Decolourization of RV 1 was recorded by measuring the absorbance at 560 nm. The % decolourization was calculated by the following equation:

$$\% \text{ Decolourization} = (A_i - A_o) / A_i \times 100, \quad (2)$$

where A_i and A_o are the initial and observed absorbance of the samples at different time intervals, respectively.

Physic-chemical parameters, i.e., temperature and pH were monitored to study the effect on decolourization of RV 1. Effect of pH on RV 1 decolourization was determined by measuring % decolourization in 2.0–7.0 pH range. The effect of temperature on decolourization of RV 1 was determined by measuring % decolourization at different temperature in the range of 20–60 °C.

Analysis of degradation metabolites

The degraded metabolites were extracted in ethyl acetate, concentrated in a rotary vacuum evaporator, and re-dissolved in a small volume of ethyl acetate. HPTLC analysis was performed to compare the R_f values of RV 1 dye and degraded metabolites on pre-coated silica gel 60 F_{254} plate. The chromatogram was observed at 254 nm using Camag TLC scanner 3. Identification of RV 1 dye and decolourized metabolites was conducted using the GC–MS/MS analysis with 30 m fused silica column (HP-5 30 m × 0.53 mm; Agilent Technologies, USA). The temperature of injection port was at 275 °C and performed at 70 eV.

Toxicity analysis of degraded metabolites

Microbial toxicity assessment of RV 1 (500 mg/l) and degraded metabolites was conducted using micro-organisms like *Bacillus subtilis*, *Streptococcus aureus*, *Salmonella typhi*, *Escherichia coli*, *Rhizobacter radiobacter*, and *Azotobacter* sp. The antibacterial action of RV 1 dye and degraded metabolites was studied using well diffusion method wherein inhibition zone surrounding the well represented the toxicity index. The phytotoxicity assessment of dye (500 and 1000 mg/l) as well as degraded metabolites was carried out on *Pennisetum glaucum* and *Vigna radiate* [24]. Ten seeds of respective plants were germinated in small pots; daily supplemented with relevant contents (distilled water, dye, or degraded metabolites) to seeds and maintaining light (12 h) and temperature (30 °C) in a controlled environment. Toxic effects were measured

in terms of % germination, plumule length, and radical length of plant after 7 days.

Results and discussion

Effect of laccase concentration cross-linking with nanosilica

To introduce primary amino-functions, reaction of TOES and NH_4OH in ethanolic solution with APTES allows the addition of amino layers on the surface of nanosilica. Glutaraldehyde molecules one side attach with laccase via amine groups of its peripheral lysine residues and amino groups of nanosilica bind on the other side. The protein content was less detected in elute while increasing the concentration of protein from 100 to 400 $\mu\text{g/ml}$. Immobilization yield of laccase nanoparticles was maximum (92%) when protein (400 $\mu\text{g/ml}$) was cross-linked with nanosilica. Maximum laccase activity was 824 U/ml on laccase nanoparticles which is shown in Fig. 1. Lack of additional bound protein with increasing protein amount (above 400 $\mu\text{g/ml}$) in the reaction mixture suggested that the surfaces of nanosilica were saturated with protein. This might be due to the formation of a dense protein layer, which caused a steric hindrance and diffusion barrier for the assessment of the enzyme on the immobilization carrier, resulting in a low immobilization yield. Similar results were reported by Al-Adhami et al. [25] wherein 1 mg/ml protein was optimum concentration for the immobilization on DEAE-Granocel support. An increase in laccase concentration from 0.25 to 2.0 mg/ml results in the increased laccase activity for the immobilization with CuTAPc- Fe_3O_4 composite [21]. Bayramoglu et al. [26] also reported adsorption capacity of CHX-g-p(IA) and CHX-g-p(IA)-Cu(II) membranes for laccase increased as the protein concentration increased from 0.1 to 1.0 mg/ml.

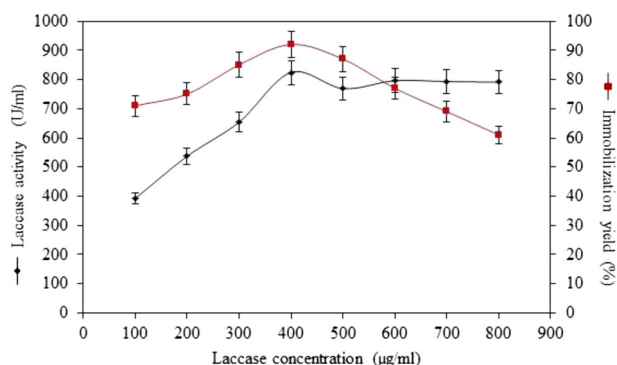


Fig. 1 Effect of laccase protein concentration on the immobilization yield

Characterization of laccase nanoparticle

The preparation of nanosilica and laccase nanoparticle was confirmed by observing micrographs on transmission electron microscope (Fig. 2a). Nanosilica had a spherical structure with smooth surfaces. It can be observed that laccase was effectively immobilized on amino-functionalized nanosilica due to their larger surface area. Thus, laccase nanoparticles showed the rough spherical surface, which can be shown in Fig. 2b. The DLS of nanosilica and laccase nanoparticles were 220 and 615 nm, respectively (Fig. 2c). The FTIR spectrum of laccase nanoparticles showed peak at 1099, 958, and 796/ cm^{-1} which corresponded to asymmetric vibration of Si–O, Si–OH, and symmetric vibration of Si–C in nanosilica and laccase nanoparticles (Fig. 3). The absorption band between 3300 and 3500 cm^{-1} is assigned to O–H stretching and H-bonded water with nanosilica [27]. The absorbance shift of nanosilica that was changed due to the laccase was cross-linked with nanosilica. The FTIR spectrum of laccase nanoparticle showed a peak at 2935/ cm^{-1} for C–H stretching, confirming cross-linking of laccase with nanosilica by glutaraldehyde molecule [28].

Temperature and pH optima

Residual activity of laccase nanoparticles on different temperature values was determined and compared to the purified laccase. A shift in the optimum temperature towards higher value was observed after cross-linking of laccase on nanosilica. The optimum temperature of purified laccase was found to be 50 $^{\circ}\text{C}$, while 55 $^{\circ}\text{C}$ was the optimum temperature for laccase nanoparticle (Fig. 4a). A shift towards the higher value may be attributed due to the use of nanosilica and their interaction with laccase. In contrast, several researchers showed that the optimum temperature was shifted towards lower temperature values [29]. Optimum temperature of free laccase and laccase immobilized Fe_3O_4 -CS-EDAC nanoparticles was 40 and 30 $^{\circ}\text{C}$, respectively. Huang et al. also stated that 55 and 45 $^{\circ}\text{C}$ were optimum temperatures for free and CuTAPc- Fe_3O_4 nanoparticle laccase, respectively [22].

The oxidation reaction for purified laccase and laccase nanoparticles had maximum activity at pH 3.0 and 4.0, respectively (Fig. 4b). Almost 15% of relative activity was retained at pH 8.0, while purified laccase was inactive. The results showed one unit shift in optimum pH towards higher value after cross-linking of laccase on nanosilica. This may be attributed due to nanosilica that has been changed micro-environment of laccase, the ionic interaction between enzyme, and charged surfaces of nanosilica. Laccase nanoparticle showed more than 90% residual activity in pH range of 3–5, while purified laccase obtained

Fig. 2 Transmission electron micrographs of **a** nanosilica, **b** laccase nanoparticle, and **c** dynamic light scattering (DLS) analysis of nanosilica and laccase nanoparticle

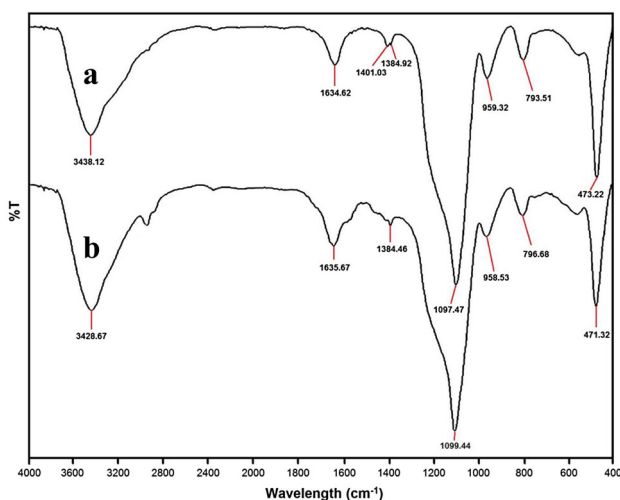
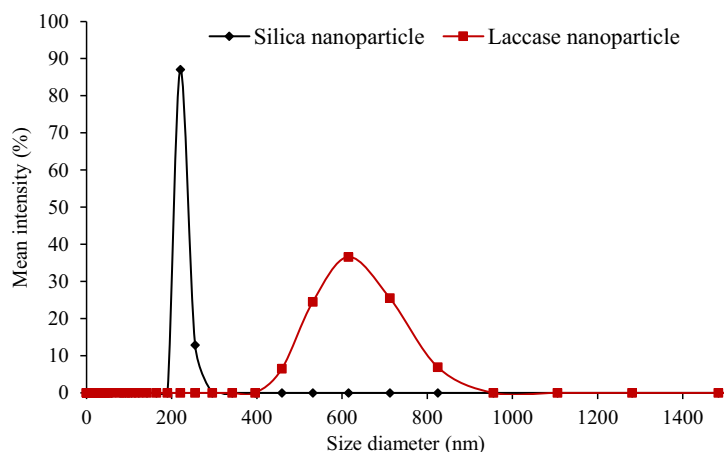
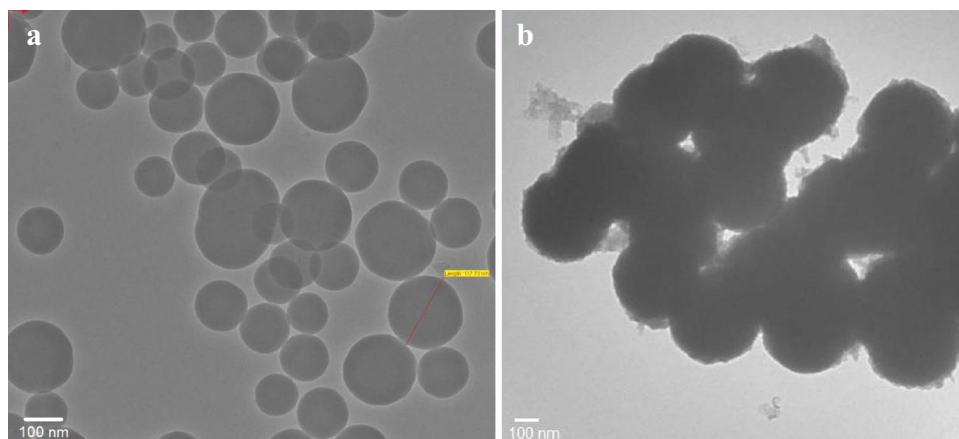


Fig. 3 Fourier transform IR spectrum of **a** nanosilica and **b** laccase nanoparticle

a comparable decrease in residual activity within the same pH range. Similarly, 0.5 and 1.5 unit shift of optimum pH after covalent immobilization of laccase on Fe₃O₄-CS-CCn and Fe₃O₄-CS-EDAC support, respectively [29]. Wang et al. [30] also reported a shift in optimum pH for the

oxidation of catechol upon immobilization of laccase on magnetic mesoporous nanosilica.

Temperature and pH stability

Purified laccase and laccase nanoparticles presented 41 and 66% of residual activity at 40 °C after 24 h, respectively (Fig. 5). The results showed that the cross-linking of laccase on nanosilica increased the stability by 25–30% in temperature range of 40–60 °C. The initial activity of purified laccase was reduced up to 75% at 70 °C within 4 h of incubation, while laccase nanoparticle showed 73% of its initial activity. Purified laccase completely inactivated at 70 °C after 24 h, while laccase nanoparticles retained 14% of initial activity. Higher temperature leads to the changes in the conformation and structure due to the breakage of bonds, thus, leading to decreased activity. The stability in laccase nanoparticles at higher temperature suggested that the exposed amine group on surface of laccase readily coupled with an aldehyde group in the nanoparticles to form a stable imine bond, which stabilizes the enzyme. When enzymes immobilized on support, materials create a kind of protection and provide a



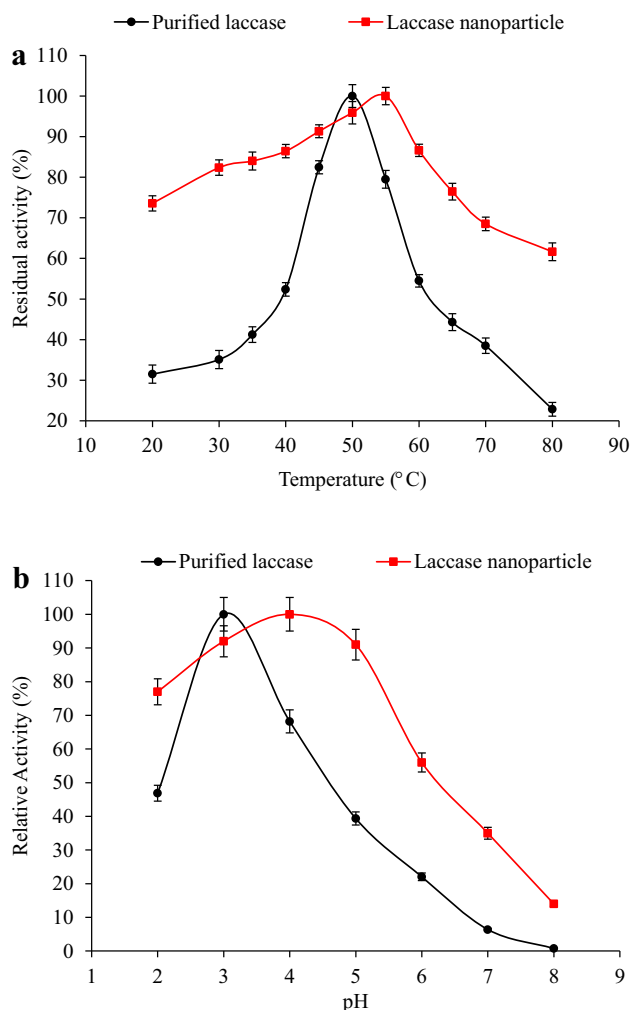


Fig. 4 Effect of temperature (a) and pH (b) on activity of purified laccase and laccase nanoparticle

resistance against the conformational changes of enzyme structure, which results in an increased thermal stability of laccase nano-conjugates [31]. Hu et al. [32] reported that laccase immobilized on nanoparticle and kaolinite was more stable as compared to the free laccase when laccase nano-conjugates incubated in a temperature range of 40–70 °C.

Laccase nanoparticles depicted more than 55% residual laccase activity at all tested pH values after 24 h of incubation, as shown in Fig. 6. Laccase nanoparticle exhibited 58% residual activity after 24 h of incubation at pH 3.0, while purified laccase depicted only 28% residual activity at the same pH. Laccase nanoparticle showed 5–10% improvement in pH stability as compared to purified laccase at pH 4.0 and 5.0. Improvement in pH stability might be observed due to the multipoint attachment of laccase on immobilization, nanosilica made laccase less prone to pH induced conformational changes. Similar results have been reported by several researchers that showed that the pH

stability of laccase was improved within pH range of 2.0–7.0 after immobilization on DEAE-Granocel 500 and sol-gel matrix, respectively [25, 33].

Storage stability of laccase nanoparticle

To store catalyst for a long time period, storage stability is a major concern. Storage stability of purified laccase and laccase nanoparticle at storage temperature of 4 and –20 °C are presented in Fig. 7a and b, respectively. The results depicted that laccase nanoparticle retained 82% of residual activity when it was stored at 4 °C for 60 days, while purified laccase retained only 44% of its initial activity. When storage temperature was –20 °C, residual activity of laccase nanoparticle and purified laccase was found to be 91% and 74%, respectively, after 60 days. Results showed that laccase nanoparticle exhibited improved storage stability as compared to purified laccase. This might be occurred due to the stability in the active conformation of laccase by multipoint interactions with amino-functionalized nanosilica. Huang et al. [22] reported 85% residual activity of a CuTAPc-Fe₃O₄ laccase nanoparticle as compared to the 30% residual activity of laccase after 30 days storage at 4 °C. Bayramoglu et al. [26] reported 37% residual activity of laccase immobilized on CHX-g-p(IA)-Cu(II) membrane after 35 days of storage at 4 °C as compared to the complete loss of the activity of laccase.

Reusability of laccase nanoparticle

Laccase is an expensive biocatalyst; the reuse of catalyst makes the enzymatic process economically viable to cut down production cost. Results depicted that more than 87.6% of laccase activity was retained till 16th cycle. Thereafter, a gradual decrease in laccase activity was observed after each cycle and almost 79% of residual activity was retained till 20th cycle (Fig. 7c). Laccase cross-linked with nanosilica was reasonably stable when repeatedly used for catalysis of ABTS oxidation. This property of laccase nanoparticle is beneficial for the application in a batch or in a continuous mode. Bayramoglu et al. [26] reported 81% residual activity of laccase immobilized on CHX-g-p(IA)-Cu(II) membrane, after 10th cycle of syringaldazine oxidation. Liu et al. [34] reported 50% residual activity of laccase immobilized on CMMC support after 10th cycle of ABTS oxidation.

Kinetic studies of laccase nanoparticle

The kinetic parameters such as K_m and V_{max} vary considerably depending upon the types of enzymes, which support materials and process conditions. Lower V_{max} may

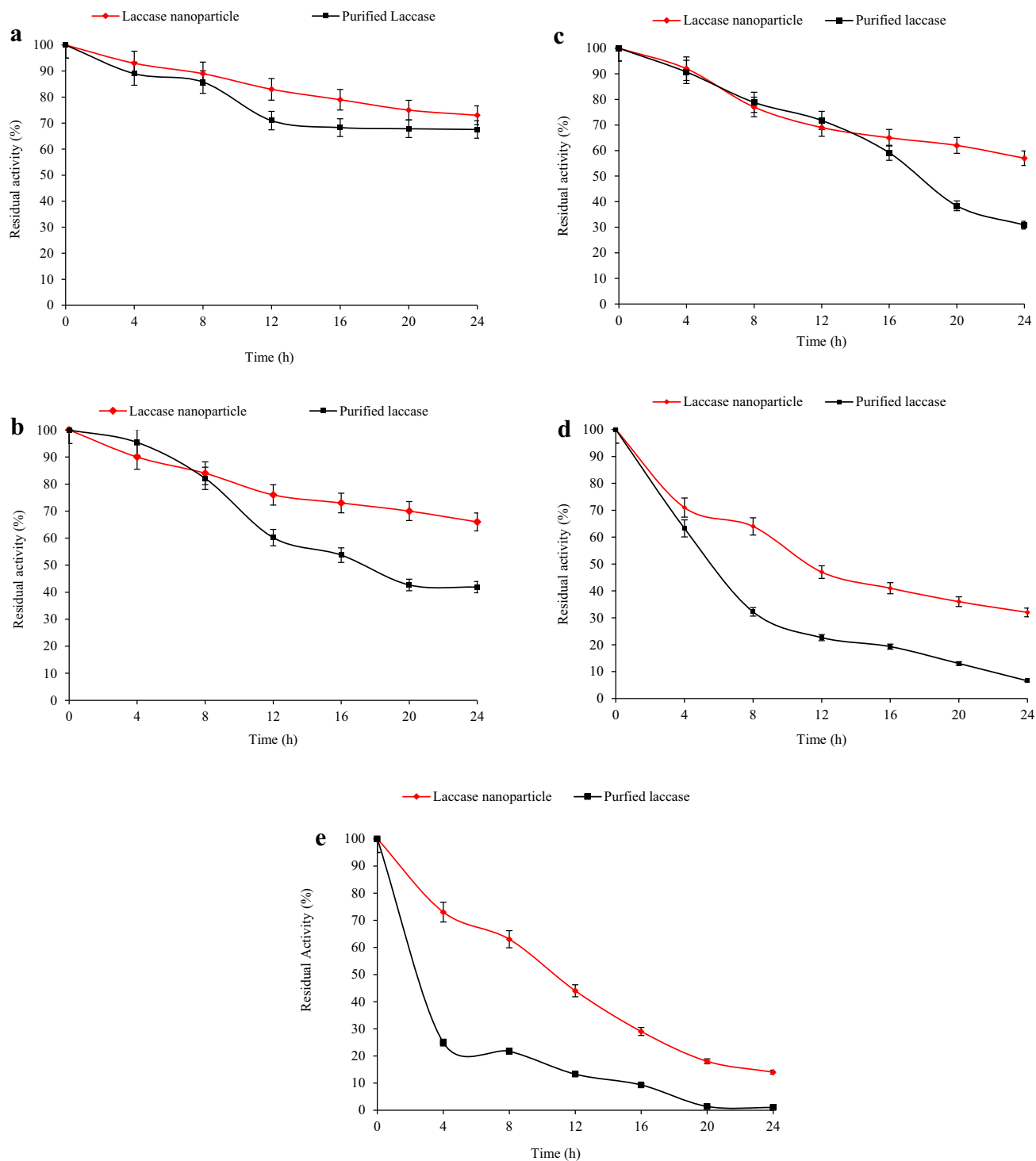


Fig. 5 Temperature stability of purified laccase and laccase nanoparticle at **a** 30 °C, **b** 40 °C, **c** 50 °C, **d** 60 °C, and **e** 70 °C

have resulted from mass transfer limitations and reduction in enzyme–substrate affinities after immobilization. Reduction in V_{\max} after laccase immobilization has also been reported by various researchers. The apparent K_m of immobilized laccase nanoparticles was found to be 0.5 mM which was 21.05% higher than purified laccase (0.19 mM).

V_{\max} of laccase nanoparticle was found to be 3.58×10^2 mM/min, which is only 29.01% of V_{\max} value of the purified laccase (12.34×10^2 mM/min). The results depicted that the catalytic efficiency of laccase nanoparticle was lower than the purified laccase. The lower catalytic efficiency of laccase nanoparticle may be due to the rigid

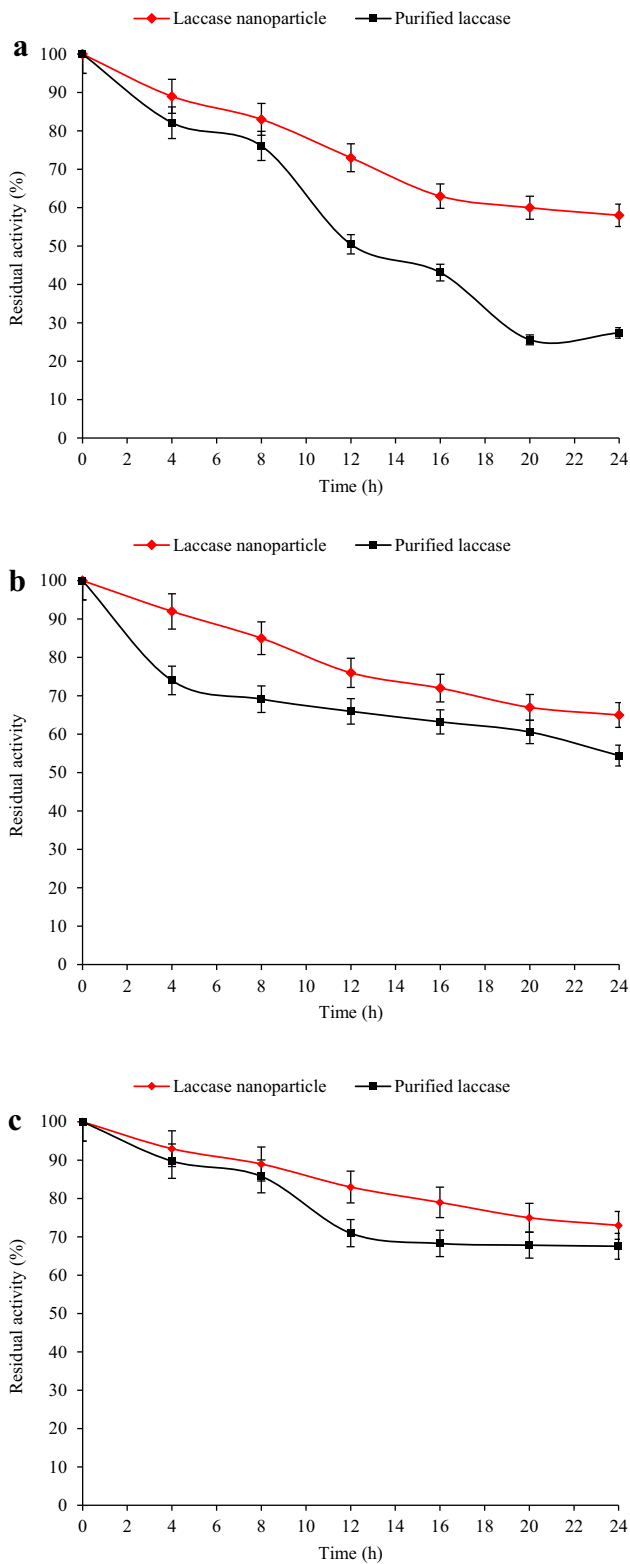


Fig. 6 pH stability purified laccase and laccase nanoparticle at **a** pH 3, **b** pH 4, and **c** pH 5

conformation of enzyme in nanoparticle form, which will not allow any changes in the conformation of active site to accommodate the substrates. When enzyme cross-linked

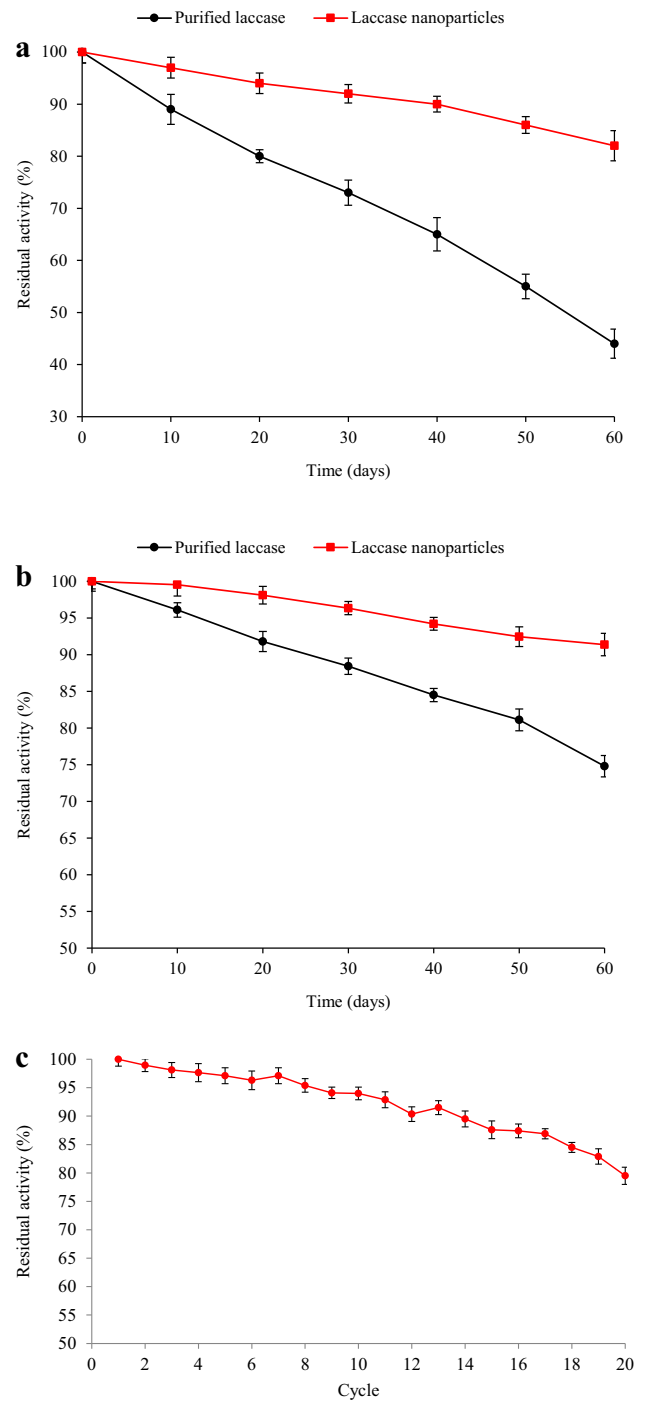


Fig. 7 Storage stability of purified laccase and laccase nanoparticle at **a** -4 °C, **b** -20 °C, and **c** reusability purified laccase and laccase nanoparticle

with nanoparticle, neighbouring enzyme molecules sterically hinder the active centres of enzyme, so all enzyme molecules may not be available for the substrates, resulting the lower catalytic efficiency of enzyme. A lower catalytic efficiency of laccase crystal had been observed by Roy et al. [35] wherein V_{max} of CLEC laccase was only 12%

than the V_{\max} of native laccase. Huang et al. [22] also reported lower catalytic efficiency of CuTAPc- Fe_3O_4 nanoparticle laccase as compared to free laccase, who reported 88.88% higher K_m and 43.33% lower V_{\max} value of CuTAPc- Fe_3O_4 nanoparticle laccase as compared to free laccase.

Decolourization of RV 1 dye using laccase nanoparticle

Incubation of RV 1 in the presence of purified laccase and immobilized silica laccase nanoparticles resulted in a detectable reduction in absorbance at 560 nm. Laccase nanoparticles showed the 66% of decolourization of dye within 4 h, while purified laccase presented 50% decolourization. Upon further incubation, 96.76% decolourization of RV 1 dye was achieved using laccase nanoparticles. The surface area of nanosilica greatly enhanced the catalytic efficiency of laccase, causing the higher decolourization of RV 1 dye (Fig. 8a). Valle-Vigón and Fuertes [36] reported 80% dye degradation of acid green 25 and remazol brilliant blue by magnetically separable carbon capsule loaded with laccase. Bayramoglu et al. [26] reported 48, 37, and 19% decolourization of methyl orange, cibron blue F3GA, and reactive black 5 dyes by *Trametes versicolour* laccase immobilized on CHX-g-p(IA)-Cu(II) membrane. Makas et al. [37] also reported 35% decolourization of methyl orange dye after 6 h treatment with laccase entrapped in semi-IPNs prepared from k-carrageenan.

Laccase nanoparticle showed more than 75% decolourization of RV 1 dye within a pH range of 3.0–6.0 (Fig. 8b). The optimum pH for dye decolourization was 4.0 wherein 96.85% of decolourization of RV 1 dye was obtained. However, decolourization of RV 1 dye was 31% at neutral (pH 7.0). Usluoglu and Arabaci [38] reported pH 4.0 as an optimum pH for maximum decolourization of acid and metal complex dyes by phenol oxidase immobilized on to alginate beads. Mogharabi et al. [39] reported pH 8.0 as optimum pH for the decolourization of dye solution of various textile dyes by laccase immobilized on alginate gelatin gel.

The optimum temperature for maximum decolourization (96.78%) of RV 1 by laccase nanoparticle was 30 °C (Fig. 8c). Decolourization of RV 1 by laccase nanoparticle was also comparable to the incubation temperature range from 25 to 50 °C. However, further increase in temperature results in the decreased decolourization of RV 1. The decrease in decolourization might be observed due to the unfolding or degradation of laccase at high temperature. Similar results have been observed by Mogharabi et al. [39] for the decolourization of crystal violet dye by laccase in alginate–gelatin mixed gel.

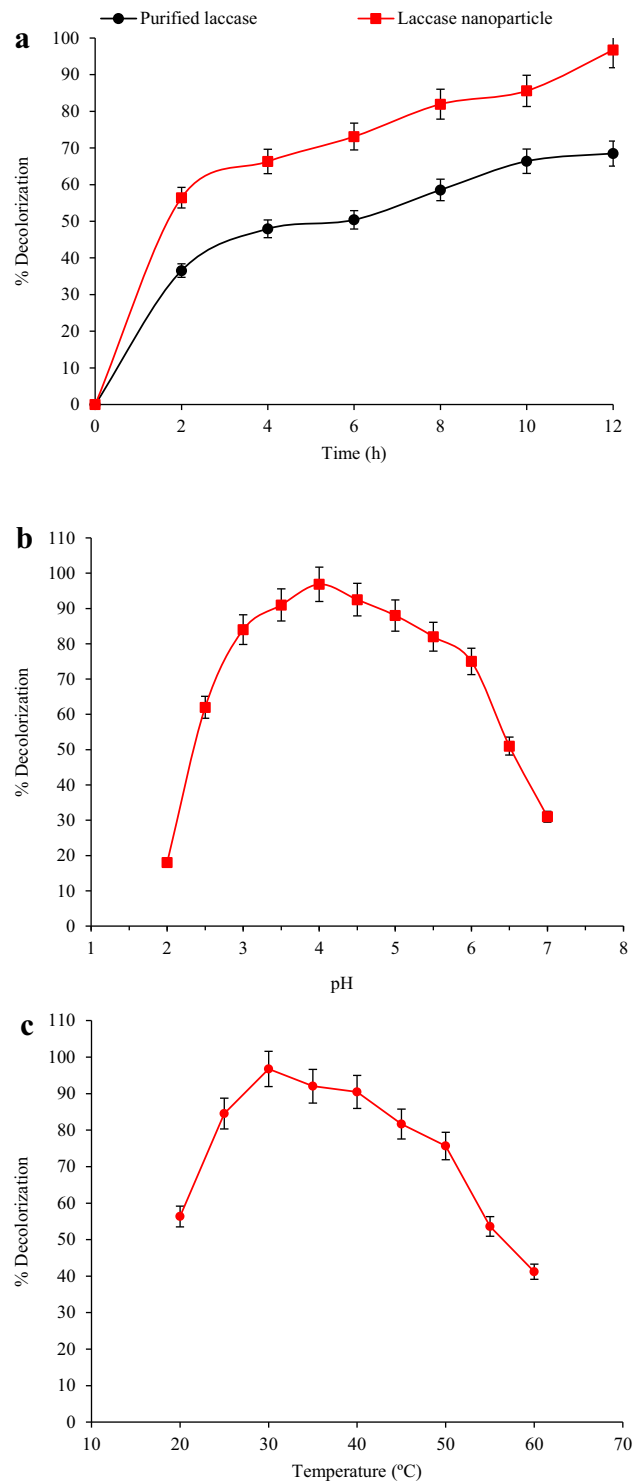


Fig. 8 Purified laccase and laccase nanoparticles were used for a decolorization of RV 1, pH (b) and temperature (c) effects were checked on the decolorization of RV 1

Analysis of degraded metabolites

The chromatogram of control dye depicted a single R_f value (0.93), while degraded metabolites showed the four

Table 1 Phytotoxicity study of untreated and laccase nanoparticle treated RV 1 dye on *V. radiata* and *P. glaucum*

Plants	<i>Vigna radiata</i>		RV1 dye (500/g)		RV1 dye (1000/g)		<i>Pennisetum glaucum</i>		RV1 dye (500/g)		RV1 dye (1000/g)	
	Control	Untreated	Treated	Untreated	Treated	Untreated	Treated	Control	Untreated	Treated	Untreated	Treated
Germination (%)	100	60	100	40	80	100	70	100	50	100	50	100
Plumule length	20.8 ± 1.3	13.5 ± 1.4	19.5 ± 1.7	11.5 ± 1.4	16.4 ± 1.5	18.9 ± 2.1	12.4 ± 1.6	16.5 ± 1.4	9.1 ± 1.1	14.4 ± 1.7	9.1 ± 1.1	14.4 ± 1.7
Radical length	6.3 ± 1.6	4.4 ± 0.9	5.6 ± 0.8	3.9 ± 0.9	4.1 ± 0.7	8.1 ± 1.4	4.2 ± 1.1	6.6 ± 1.1	3.2 ± 0.8	5.1 ± 1.7	3.2 ± 0.8	5.1 ± 1.7

depicted almost similar inhibition zone. Growth of *B. cereus* and *Azotobacter* sp. was unaffected when both bacteria were tested against degraded metabolites of Synozol red HF-6BN using *Aspergillus niger* and *Nigrospora* sp. [42].

Vigna radiata seeds were treated with 500 and 1000 mg/l concentration of RV 1 dye, the germination rate was 90 and 40%, respectively. In contrast, treatment with degraded products of the same concentration had a minor effect on plants, as germination rates were 100 and 80%, plumule lengths were 19.5 ± 1.7 and 16.4 ± 1.5 cm, and radical lengths were found to be 5.6 ± 0.8 and 4.1 ± 0.7 cm, respectively. Treatment of *Pennisetum glaucum* seeds with RV 1 dye (500 and 1000 mg/l) resulted in lower germination (80 and 50%, respectively) in plant seeds (Table 1). Seed germination of degraded metabolites depicted the lower inhibition than control dye samples, suggesting the non-toxic nature of degraded metabolites. Non-toxic nature of degraded metabolite of Rubine GFL dye sample and textile effluents was observed for germination of *S. vulgare* and *P. mungo* seeds as compared to original dye and textile effluent samples [43].

Conclusions

Overall, amino-functionalized nanosilica was synthesized chemically and anchored covalently using glutaraldehyde to laccase enzyme. Due to the immobilization with nanosilica, laccase nanoparticles obtained higher efficiency at higher pH and temperature compared to purified laccase. Laccase nanoparticles displayed higher stability with repeated use, long-term storage, and thermal stability than purified laccase. Furthermore, prepared nano-conjugates efficiently cleaved RV 1 dye and transformed into less-toxic products, which represented an additional advantage for waste water treatment. Though laccase nanoparticles obtained lower catalytic efficiency than purified laccase, laccase nanoparticles are promising biocatalysts that can be used for the elimination of synthetic dyes.

Acknowledgements The authors are very obliged to the Department of Biotechnology (DBT Sanction No. BT/PR9134/BCE/08/543/2007) and Ministry of Science and Technology, New Delhi, for their financial support. The authors also wish to acknowledge SICART, V.V. Nagar, Gujarat, for providing the necessary instrumentation facilities.

Open Access This article is distributed under the terms of the Creative Commons Attribution 4.0 International License (<http://creativecommons.org/licenses/by/4.0/>), which permits unrestricted use, distribution, and reproduction in any medium, provided you give appropriate credit to the original author(s) and the source, provide a link to the Creative Commons license, and indicate if changes were made.

References

- Rao, M., Scelza, R., Acevedo, F., Diez, M., Gianfreda, L.: Enzymes as useful tools for environmental purposes. *Chemosphere* **107**, 145–162 (2014)
- Avvakumova, S., Colombo, M., Tortora, P., Prosperi, D.: Biotechnological approaches toward nanoparticle biofunctionalization. *Trends Biotechnol.* **32**, 11–20 (2014)
- Mukhopadhyay, A., Dasgupta, A.K., Chakrabarti, K.: Enhanced functionality and stabilization of a cold active laccase using nanotechnology based activation-immobilization. *Bioresour. Technol.* **179**, 573–584 (2015)
- Lettera, V., Pezzella, C., Cicatiello, P., Piscitelli, A., Giacobelli, V.G., Galano, E., Amoresano, A., Sannia, G.: Efficient immobilization of a fungal laccase and its exploitation in fruit juice clarification. *Food Chem.* **196**, 1272–1278 (2016)
- Cipolatti, E.P., Silva, M.J.A., Klein, M., Feddern, V., Feltes, M.M.C., Oliveira, J.V., Ninow, J.L., de Oliveira, D.: Current status and trends in enzymatic nanoimmobilization. *J. Mol. Catal. B Enzym.* **99**, 56–67 (2014)
- da Costa, J.P., Oliveira-Silva, R., Daniel-da-Silva, A.L., Vitorino, R.: Bionanoconjugation for proteomics applications—an overview. *Biotechnol. Adv.* **32**, 952–970 (2014)
- Min, K., Yoo, Y.J.: Recent progress in nanobiocatalysis for enzyme immobilization and its application. *Biotechnol. Bioproc. E.* **19**, 553–567 (2014)
- Yang, H.W., Hua, M.Y., Chen, S.L., Tsai, R.Y.: Reusable sensor based on high magnetization carboxyl-modified graphene oxide with intrinsic hydrogen peroxide catalytic activity for hydrogen peroxide and glucose detection. *Biosens. Bioelectron.* **41**, 172–179 (2013)
- Hou, J., Dong, G., Ye, Y., Chen, V.: Laccase immobilization on titania nanoparticles and titania-functionalized membranes. *J. Membr. Sci.* **452**, 229–240 (2014)
- Ding, S., Cargill, A.A., Medintz, I.L., Claussen, J.C.: Increasing the activity of immobilized enzymes with nanoparticle conjugation. *Curr. Opin. Biotechnol.* **34**, 242–250 (2015)
- Kües, U.: Fungal enzymes for environmental management. *Curr. Opin. Biotechnol.* **33**, 268–278 (2015)
- Senthivelan, T., Kanagaraj, J., Panda, R.: Recent trends in fungal laccase for various industrial applications: an eco-friendly approach—A review. *Biotechnol. Bioproc. E.* **21**, 19–38 (2016)
- Asif, M.B., Hai, F.I., Singh, L., Price, W.E., Nghiem, L.D.: Degradation of pharmaceuticals and personal care products by white-rot fungi—a critical review. *Curr. Pollut. Rep.* **3**(2), 88–103 (2017)
- Fernández-Fernández, M., Sanromán, M.Á., Moldes, D.: Recent developments and applications of immobilized laccase. *Biotechnol. Adv.* **31**, 1808–1825 (2013)
- Catherine, H., Penninckx, M., Frédéric, D.: Product formation from phenolic compounds removal by laccases: a review. *Environ. Technol. Innov.* **5**, 250–266 (2016)
- Pang, R., Li, M., Zhang, C.: Degradation of phenolic compounds by laccase immobilized on carbon nanomaterials: diffusional limitation investigation. *Talanta* **131**, 38–45 (2015)
- Richter, M., Schulenburg, C., Jankowska, D., Heck, T., Faccio, G.: Novel materials through nature's catalysts. *Mater. Today* **18**, 459–467 (2015)
- Li, Q.Y., Wang, P.Y., Zhou, Y.L., Nie, Z.R., Wei, Q.: A magnetic mesoporous SiO₂/Fe₃O₄ hollow microsphere with a novel network-like composite shell: synthesis and application on laccase immobilization. *J. Sol Gel Sci. Technol.* **78**, 523–530 (2016)
- Asther, M., Lesage, L., Drapron, R., Corrieu, G., Odier, E.: Phospholipid and fatty acid enrichment of *Phanerochaete chrysosporium* INA-12 in relation to ligninase production. *Appl. Microbiol. Biot.* **27**, 393–398 (1988)
- Rudakiya, D.M., Gupte, A.: Degradation of hardwoods by treatment of white rot fungi and its pyrolysis kinetics studies. *Int. Biodeter. Biodegr.* **120**, 21–35 (2017)
- Stöber, W., Fink, A., Bohn, E.: Controlled growth of monodisperse silica spheres in the micron size range. *J. Colloid Interface Sci.* **26**, 62–69 (1968)
- Huang, J., Xiao, H., Li, B., Wang, J., Jiang, D.: Immobilization of *Pycnoporus sanguineus* laccase on copper tetra-aminophthalocyanine-Fe₃O₄ nanoparticle composite. *Biotechnol. Appl. Bioc.* **44**, 93–100 (2006)
- Lowry, O.H., Rosebrough, N.J., Farr, A.L., Randall, R.J.: Protein measurement with the Folin phenol reagent. *J. Biol. Chem.* **193**, 265–275 (1951)
- Kalme, S., Jadhav, S., Parshetti, G., Govindwar, S.: Biodegradation of Green HE4B: co-substrate effect, biotransformation enzymes and metabolite toxicity analysis. *Indian J. Microbiol.* **50**, 156–164 (2010)
- Al-Adhami, A.J., Bryjak, J., Greb-Markiewicz, B., Peczyńska-Czoch, W.: Immobilization of wood-rotting fungi laccases on modified cellulose and acrylic carriers. *Process Biochem.* **37**, 1387–1394 (2002)
- Bayramoglu, G., Gursel, I., Yilmaz, M., Arica, M.Y.: Immobilization of laccase on itaconic acid grafted and Cu (II) ion chelated chitosan membrane for bioremediation of hazardous materials. *J. Chem. Technol. Biot.* **87**, 530–539 (2012)
- Beganskienė, A., Sirutkaitis, V., Kurtinaitienė, M., Juškėnas, R., Kareiva, A.: FTIR, TEM and NMR investigations of Stöber silica nanoparticles. *Mater. Sci.* **10**, 287–290 (2004)
- Rudakiya, D.M., Pawar, K.: Bactericidal potential of silver nanoparticles synthesized using cell-free extract of *Comamonas acidovorans*: in vitro and in silico approaches. *3 Biotech* **7**(2), 92 (2017)
- Kalkan, N.A., Aksoy, S., Aksoy, E.A., Hasirci, N.: Preparation of chitosan-coated magnetite nanoparticles and application for immobilization of laccase. *J. Appl. Polym. Sci.* **123**, 707–716 (2012)
- Wang, F., Guo, C., Yang, L.R., Liu, C.Z.: Magnetic mesoporous silica nanoparticles: fabrication and their laccase immobilization performance. *Bioresour. Technol.* **101**, 8931–8935 (2010)
- Cabana, H., Ahamed, A., Leduc, R.: Conjugation of laccase from the white rot fungus *Trametes versicolor* to chitosan and its utilization for the elimination of triclosan. *Bioresour. Technol.* **102**, 1656–1662 (2011)
- Hu, X., Zhao, X., Hwang, H.M.: Comparative study of immobilized *Trametes versicolor* laccase on nanoparticles and kaolinite. *Chemosphere* **66**, 1618–1626 (2007)
- Irshad, M., Bahadur, B.A., Anwar, Z., Yaqoob, M., Ijaz, A., Iqbal, H.M.N.: Decolorization applicability of sol-gel matrix-immobilized laccase produced from *Ganoderma leucidum* using agro-industrial waste. *BioResources* **7**, 4249–4261 (2012)
- Liu, Y., Zeng, Z., Zeng, G., Tang, L., Pang, Y., Li, Z., Liu, C., Lei, X., Wu, M., Ren, P.: Immobilization of laccase on magnetic bimodal mesoporous carbon and the application in the removal of phenolic compounds. *Bioresour. Technol.* **115**, 21–26 (2012)
- Roy, J.J., Abraham, T.E., Abhijith, K., Kumar, P.S., Thakur, M.: Biosensor for the determination of phenols based on cross-linked enzyme crystals (CLEC) of laccase. *Biosens. Bioelectron.* **21**, 206–211 (2005)
- Valle-Vigón, P., Fuertes, A.B.: Magnetically separable carbon capsules loaded with laccase and their application to dye degradation. *RSC Adv.* **1**, 1756–1762 (2011)
- Makas, Y.G., Kalkan, N.A., Aksoy, S., Altinok, H., Hasirci, N.: Immobilization of laccase in κ-carrageenan based semi-



- interpenetrating polymer networks. *J. Biotechnol.* **148**, 216–220 (2010)
38. Usluoglu, A., Arabaci, G.: Dye decolourization by Dandelion (*Taraxacum officinale*) polyphenol oxidase immobilized into alginate beads. *Res. J. Chem. Environ.* **17**, 16–20 (2013)
39. Mogharabi, M., Nassiri-Koopaei, N., Bozorgi-Koushalshahi, M., Nafissi-Varcheh, N., Bagherzadeh, G., Faramarzi, M.A.: Immobilization of laccase in alginate-gelatin mixed gel and decolourization of synthetic dyes. *Bioinorg. Chem. Appl.* 1–6 (2012). doi:[10.1155/2012/823830](https://doi.org/10.1155/2012/823830)
40. Zille, A., Górnacka, B., Rehorek, A., Cavaco-Paulo, A.: Degradation of azo dyes by *Trametes villosa* laccase over long periods of oxidative conditions. *Appl. Environ. Microb.* **71**, 6711–6718 (2005)
41. Jadhav, S.B., Phugare, S.S., Patil, P.S., Jadhav, J.P.: Biochemical degradation pathway of textile dye Remazol red and subsequent toxicological evaluation by cytotoxicity, genotoxicity and oxidative stress studies. *Int. Biodeter. Biodegr.* **65**, 733–743 (2011)
42. Ilyas, S., Rehman, A.: Decolourization and detoxification of Synozol red HF-6BN azo dye, by *Aspergillus niger* and *Nigrospora sp.* *Iran J. Environ. Health Sci Eng.* **10**(1), 12 (2013)
43. Lade, H.S., Waghmode, T.R., Kadam, A.A., Govindwar, S.P.: Enhanced biodegradation and detoxification of disperse azo dye Rubine GFL and textile industry effluent by defined fungal-bacterial consortium. *Int. Biodeter. Biodegr.* **72**, 94–107 (2012)

